

Fluticasone propionate suppresses the SARS-CoV-2 induced increase in respiratory epithelial permeability in vitro*

Katleen Martens^{1,2,#}, Emiel Vanhulle^{3,#}, An-Sofie Viskens¹, Brecht Steelant¹, Peter W. Hellings^{1,4,5}, Kurt Vermeire³

Rhinology 61: 2, 161 - 169, 2023
<https://doi.org/10.4193/Rhin22.223>

¹ Department of Microbiology, Immunology and Transplantation, Allergy and Clinical Immunology Research Unit, KU Leuven, Leuven, Belgium

² Department of Bioscience Engineering, University of Antwerp, Antwerp, Belgium

³ KU Leuven Department of Microbiology, Immunology and Transplantation, Rega Institute for Medical Research, Laboratory of Virology and Chemotherapy, KU Leuven, Leuven, Belgium

⁴ University Hospitals Leuven, Clinical Department of Otorhinolaryngology, Head and Neck Surgery, Leuven, Belgium

⁵ Department of Otorhinolaryngology, Academic Medical Center, University of Amsterdam, Amsterdam, the Netherlands

***Received for publication:**
June 10, 2022

Accepted: November 28, 2022

Shared first authorship

Abstract

Background: Disruption of the nasal epithelial barrier is believed to play a role in Coronavirus Disease-2019 (COVID-19) outcomes. Fluticasone propionate has been shown to restore the nasal epithelial barrier in allergic rhinitis to the level of healthy controls. The therapeutic potential of nasal steroid sprays in COVID-19 has recently been reported. However, further insight into the mode of action is warranted.

Objectives: To explore the in vitro mechanisms of the preventive potential of fluticasone propionate in SARS-CoV-2 infection.

Methods: Human air liquid interface cultures of Calu-3 cells and primary nasal epithelial cells isolated from healthy donors were used to investigate the preventive effect of fluticasone propionate on SARS-CoV-2 induced barrier disruption, virus replication and ACE2 expression.

Results: 48 hours pre-treatment with fluticasone propionate prevented the SARS-CoV-2 induced increase in fluorescein isothiocyanate-dextran 4 kDa permeability and reduced infection with SARS-CoV-2. Pre-treatment with fluticasone propionate also decreased ACE2 expression in SARS-CoV-2 infected Calu-3 cells.

Conclusion: Fluticasone propionate pre-treatment prevented SARS-CoV-2 increased epithelial permeability, reduced ACE2 expression and SARS-CoV-2 infection, underscoring the therapeutic potential of fluticasone propionate in the context of COVID-19.

Key words: SARS-CoV-2; Fluticasone propionate; epithelial permeability; ACE2; viral release

Introduction

Coronavirus Disease-2019 (COVID-19) has caused a substantial pandemic, posing a serious threat to international health care systems^(1,2). The several vaccines that have already been approved or that are currently under development, seem insufficient to halt the spread of newly arising SARS-CoV-2 variants⁽³⁾ and will most likely not be sufficient to prevent future waves of SARS-CoV-2 infection worldwide. In addition, the lack of specific treatment strategies for SARS-CoV-2 is a risk that should not

be underestimated^(4,5). The identification of new and effective compounds against SARS-CoV-2 is therefore highly warranted^(1,2), with a clear distinction between the preventive and curative potential of the antivirals at the different stages of disease.

The respiratory tract is continuously exposed to various environmental substances, making it a primary target for SARS-CoV-2 to enter and infect the human body⁽⁶⁾. The integrity of the epithelial barrier towards environmental insults is preserved by

tight junctions (TJs), adherens junctions (AJs) and desmosomes that contribute to sealing intracellular spaces, among other functions⁽⁷⁾. These junctions consist of a complex architecture of polymorphic transmembrane proteins (e.g., occludin) that through adaptor proteins (e.g., zonula occludens 1) interact with the cytoskeleton⁽⁷⁾. Consequently, exposure to harmful agents can lead to a leaky epithelial barrier and induction of airway inflammation. Furthermore, disruption of the epithelial barrier by viral infection is believed to be an important driver of respiratory exacerbations⁽⁸⁻¹⁰⁾. For instance, in vitro and in vivo studies have shown that respiratory syncytial virus infection can disrupt airway epithelial barrier integrity⁽⁹⁻¹¹⁾. In addition, Hao et al. demonstrated that long-term infection of human airway epithelial cells with SARS-CoV-2 resulted in dispersed zonula occludens-1 expression without clear tight junctions and partial loss of cilia, which lead to damage of the human airway epithelium⁽⁸⁾. The importance of the epithelium as entry site for SARS-CoV-2 infection has also been documented by several reports showing enriched angiotensin-converting enzyme 2 (ACE2) expression, the main receptor for this virus, in nasal epithelial cells^(12,13). Indeed, SARS-CoV-2 relies heavily on ACE2 and transmembrane protease serine 2 (TMPRSS2) expression for cell entry⁽¹⁴⁾. More specifically, SARS-CoV-2 binds to ACE2 expressed on human airway epithelial cells, followed by cleavage and activation of the viral spike protein by the serine protease TMPRSS2. These cellular receptors ultimately facilitate virus-cell fusion and cell entry⁽¹⁴⁾. Very recently, ACE2 has been reported to have different expression levels in airways under distinct chronic inflammatory airway diseases, such as chronic obstructive pulmonary disease (COPD), allergic asthma and chronic rhinosinusitis, which may be associated with COVID-19 risk⁽¹⁵⁾. Altogether, these findings further highlight the important role of the nasal mucosa in the infection process of SARS-CoV-2.

A recent study by Strauss et al. has pointed towards the benefits of nasal corticosteroid sprays in COVID-19 infected individuals, with a significant reduction of severe illness, hospitalization rates and intensive care unit administrations⁽¹⁶⁾. Inhaled corticosteroids (ICS) are a standard anti-inflammatory therapy to treat a wide range of chronic airway diseases, such as chronic rhinosinusitis, respiratory allergies, and asthma⁽¹⁷⁾. Our research group has previously demonstrated that nasal corticosteroid molecules, such as fluticasone propionate (FP), can protect the airway epithelium from external and internal damage^(18,19). It is hypothesized that ICS may reduce expression of the ACE2 receptor in epithelial cells, through suppression of Type-I interferon response, and thus contribute to altered susceptibility to infection with SARS-CoV-2⁽²⁰⁾.

In this study we aim to demonstrate the preventive effect of FP on SARS-CoV-2 infection. Using human air-liquid interface (ALI) cultures of Calu-3 cells and primary nasal epithelial cells (pNECs)

isolated from healthy donors, we demonstrated that a 48 hours pre-treatment with FP suppresses SARS-CoV-2 induced barrier disruption, and, was associated with downregulation of ACE2 expression.

Methods

Study approval

All experiments were approved by the Medical Ethical Committee of the University Hospitals Leuven (S65483).

Cell lines and viruses

Cell lines

African green monkey kidney cells (Vero E6 cells) were obtained from ATCC (CRL-1586) (Manassas, VA, USA) as mycoplasma-free stocks and were grown in Dulbecco's Modified Eagle Medium (DMEM, Thermo Fisher Scientific (TFS), Merelbeke, Belgium) supplemented with 10% fetal bovine serum (FBS), 2 mM L-glutamine (TFS) and 0.075% sodium-bicarbonate (TFS). End-point titrations on Vero E6 cells were performed with medium containing 2% FBS instead of 10%. Cells were maintained at 37°C in a humidified environment with 5% CO₂ and were passaged every 3 to 4 days.

Viruses

All virus-related work was conducted in the high-containment biosafety level 3 facilities of the Rega Institute from the KU Leuven (Leuven, Belgium), according to institutional guidelines. Severe Acute Respiratory Syndrome coronavirus 2 isolates (SARS-CoV-2) were recovered from nasopharyngeal swabs of RT-qPCR-confirmed human cases obtained from the University Hospital Leuven (Leuven, Belgium).

SARS-CoV-2 viral stock was prepared by inoculation of confluent Vero E6 cells as described in detail in a recent published article⁽²¹⁾. Recombinant SARS-CoV-2-GFP virus (Wuhan strain), as described in⁽²²⁾, was a kind gift from Dr. Volker Thiel (University of Bern, Switzerland).

Isolation of primary nasal epithelial cells from inferior turbinate

Inferior turbinate of patients (n=4) undergoing aesthetic and/or functional rhinoplasty for an anatomical problem and not mucosal disease, was used for isolation of primary epithelial cells. Patient demographics are depicted in Table E1. A highly purified epithelial cell population was obtained as reported previously⁽¹⁸⁾. In brief, inferior turbinates were enzymatically digested in 0.1% pronase (Protease XIV, Sigma, Hoeilaart, Belgium) solution in DMEM-F12 culture medium supplemented with 100 U/ml penicillin, 100 µg/ml streptomycin, and 2% Ultrosor G (Pall Life Sciences, Merelbeke, Belgium). After overnight incubation at 4°C while shaking, the protease reaction was stopped by the addition of fetal bovine serum (FBS) (10%). Cells were washed

in culture medium and pelleted by centrifugation for 5 min at 100 g. Cells were then resuspended in 10 ml culture medium and incubated in a plastic culture flask for one hour at 37°C to remove fibroblasts. The cell suspension was mixed with 2×10^7 prewashed CD45- and CD15-magnetic beads (Dynabeads®, Invitrogen) and epithelial cells were purified by negative selection following the manufacturer's instructions.

Air-liquid interface cultures

Primary nasal epithelial cells

Primary nasal epithelial cells from healthy controls (n=4) were grown in bronchial epithelial basal medium (Lonza, Basel, Switzerland) supplemented with the SingleQuot Kit, in a T75 culture flask at 37°C. Once cells reached 75-80% confluency, cells were detached and were seeded on 6.5 mm diameter polyester transwell inserts (Costar; Corning, Corning, NY, USA) at a density of 100.000 cells/well. Cells were grown submerged for 7 days until a confluent monolayer was formed. Afterwards, cells were placed in ALI for 21 days to further differentiate the cells. Primary nasal epithelial cells were cultured in DMEM-F12 culture medium supplemented with 100 U/ml penicillin, 100 µg/ml streptomycin, and 2% Ultrosor G (Pall Life Sciences). Medium of the primary nasal epithelial cells was changed every other day.

Calu-3 cells

Calu-3 cells (n=4) were grown in EMEM medium (Lonza), supplemented with 10% FBS, 1% L-glutamine and 100 U/ml penicillin, 100 µg/ml streptomycin in a T75 culture flasks. Calu-3 cells between passages 10-15 were used. Once cells reached 75-80% confluency, cells were detached and were seeded on 6.5 mm diameter polyester transwell inserts (Costar; Corning) at a density of 100.000 cells/well. Cells were grown submerged for 7 days until a confluent monolayer was formed. Afterwards, cells were placed in ALI for 21 days to further differentiate the cells. Medium of the Calu-3 cells was changed every other day.

Paracellular flux measurements

Fluorescein isothiocyanate dextran 4 kDa (FD4) (Sigma-Aldrich, St Louis, MI, USA) was used to measure epithelial permeability. FD4 (2 mg/mL) was added apically to the ALI cultures 24 hours post infection and the fluorescein isothiocyanate intensity of basolateral fluid was measured using a fluorescence reader (FLUOstar Omega; BMG Labtech, Ortenberg, Germany). FD4 concentration was calculated and is relatively expressed.

Stimulation experiments of primary nasal and Calu-3 epithelial cell cultures

Fluticasone propionate (FP 0,1 µM) was applied basolaterally to ALI cultures of primary nasal epithelial cells and Calu-3 cells 48 hours and 24 hours prior to SARS-CoV-2 infection. On day zero, ALI cultures were infected apically with Recombinant SARS-CoV-

2-GFP virus (Wuhan strain; 100 µl, MOI of 0.2). After 2 hours of infection, inoculum (virus) was removed, and inserts were then washed apically with PBS to remove remaining virus. At different timepoints post infection (24, 48 and 72 hours), 150 µl of basolateral medium was collected to determine viral yield basolaterally and inserts were also apically washed with PBS to determine viral yield. In addition, FD4 (2 mg/ml) was added 24 hours after infection, apically to evaluate permeability. 48 hours and 72 hours post infection, 100 µl of basolateral medium was collected to determine FD4 permeability.

mRNA isolation and RT-qPCR ACE2 expression

RNA from Calu-3 cells and PNECs was isolated with the Qiagen Mini RNeasy kit (Germantown, MD, USA) and 1 µg of total RNA was reversed transcribed into cDNA with the High-Capacity cDNA Reverse Transcription Kit (Applied Biosystems) according to manufacturer's protocol. cDNA plasmid standards, consisting of purified plasmid DNA specific for each individual target, were used to quantify the target gene in the unknown samples. The housekeeping genes to normalize ACE2 expression in ALI cultures were PPIA and RACK1. The primer and probe sequences for the specific genes were determined in the laboratory of Clinical Immunology using Primer Express (Applied Biosystems). RT-qPCR was performed in an CFX Connect (Bio-Rad Laboratories Inc, Hercules, CA, USA) for all genes with specific Taqman probes and primers and using Platinum® Quantitative PCR SuperMix-UDG w/ROX (TFS). Sequences for the probes and primers can be found in Table E2.

Viral RNA extraction and RT-qPCR SARS-CoV-2

Total RNA was extracted from both apical washes and from basolateral medium collections using QIAamp viral RNA mini kit (Qiagen) following manufacturer's instruction.

The duplex RT-qPCR assay used for the detection of SARS-CoV-2 envelope (E) and nucleocapsid (N) gene has been described in detail before ⁽²¹⁾.

Briefly, all primers and probes were obtained from Integrated DNA Technologies (IDT, Leuven, Belgium). Final concentration of combined primer/probe mix consist of 500 nM forward and reverse primer and 250 nM probe. Viral E and N genes are simultaneously amplified and tested using a multiplex RT-qPCR. All the procedures follow the manufacturer's instructions of the Applied Biosystems TaqMan Fast Virus one-step mastermix (TFS). qPCR plate was read in the FAM and HEX channels using a QuantStudio™ 5 Real-Time PCR system (TFS) under the following cycling protocol: 50°C for 5 min, 95°C for 20 seconds, followed by 45 cycles of 95°C for 3 seconds and 55°C for 30 seconds. A stabilized in vitro transcribed universal synthetic single stranded RNA of 880 nucleotides in buffer with known copy number concentration (Joint Research Centre, European Commission, Cat. n° EURM-019) was used as a standard to quantitatively measure

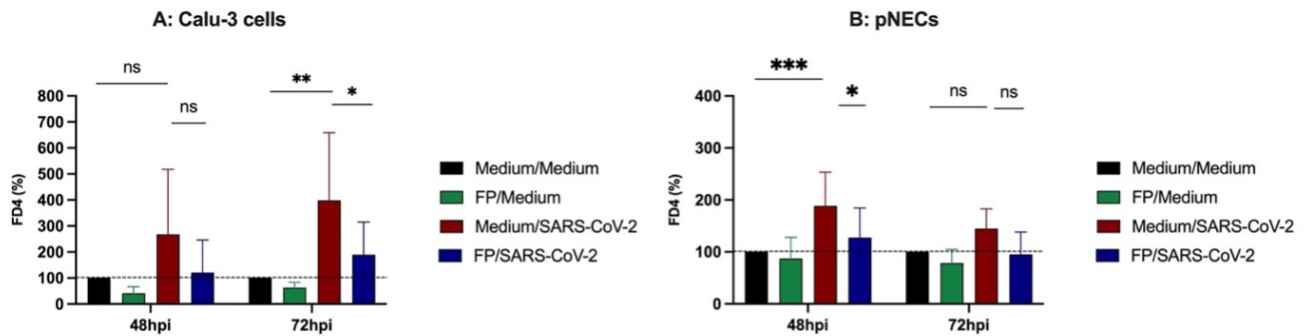


Figure 1. FP treatment prevents SARS-CoV-2 induced barrier disruption in vitro. A-B: FD4 levels were quantified at 48 hours and 72 hours post infection. Data are shown as mean \pm SD. Bars show FD4 values, expressed as % relative to medium control. Significance was calculated by using two-way ANOVA with post-hoc analysis. * P <0.05, ** P <0.01, *** P <0.001, ns = not significant.

viral copy numbers.

Immunofluorescence microscopy

ALI cultures of both primary nasal epithelial and Calu-3 cells were infected with a GFP gene-coupled SARS-CoV-2 variant for 2 hours and microscopic images were taken at different time points post infection (24, 48 and 72 hours). At designated timepoints, these ALI cultures were imaged with a Primovert iLED inverted immunofluorescence microscope employing a 4X Plan-Achromat objective coupled to a Axiocam 202 mono microscope camera (Zeiss NTS Ltd). Representative images of four different experiments were captured in the green channel of the microscope. GFP expression was then quantified, and images were further processed and analyzed using the open-source image analysis software Fiji⁽²³⁾. In brief, images were added to a stack and converted to 8-bit. A threshold was set to separate background from GFP positive signal. GFP⁺ area was measured as a percentage of the total cell area⁽²⁴⁾.

Statistics

Data were analyzed using Graphpad Prism software version 10 (La Jolla, CA, USA). Differences were considered significant at p value < 0.05. Differences between two groups were evaluated by using a student's t -test or the Mann-Whitney U test depending on normality. For differences between multiple groups, One-Way ANOVA or Kruskal-Wallis test with post hoc.

Results

Fluticasone propionate suppresses SARS-CoV-2 induced increase in FD4 permeability

Firstly, we evaluated the impact of SARS-CoV-2 infection on cell barrier integrity and tested the preventive effect of FP on permeability of SARS-CoV-2 infected cell cultures. Two different cell cultures were investigated in parallel, i.e., primary nasal epithelial cells (pNECs) of healthy individuals, and, the bronchial epithelial cell line, Calu-3 cells⁽¹⁹⁾. Patient characteristics are

depicted in Table E1 in this article's Online repository. Briefly, Calu-3 cells and pNECs were cultured in ALI on transwell inserts for 21 days, as described previously⁽¹⁸⁾. Next, cells were treated basolaterally with FP for 48 hours prior to SARS-CoV-2 infection, and FITC-dextran 4kDa (FD4) permeability was evaluated 48 and 72 hours post infection. Our results showed that SARS-CoV-2 infection of ALI cultures induced a significant increase in epithelial permeability, as measured by FD4 transport, both in Calu-3 cells (Figure 1A) as in pNECs (Figure 1B). Importantly, basolateral pre-treatment with FP significantly suppressed the SARS-CoV-2 induced increase in FD4 passage at 72 hours post infection in Calu-3 cells (Figure 1A). In pNECs, FP clearly reduced the SARS-CoV-2 induced increase in FD4 levels reaching significance for the samples taken at 48 hours post infection (Figure 1B). As the permeability of the epithelial barrier towards environmental insults is preserved by tight junctions (TJ), among others, we investigated the effect of SARS-CoV-2 infection on TJ expression (i.e., occludin, zonula occludens-1, claudin-1, -3 and -4) in Calu-3 cells 72 hours post infection. We found that SARS-CoV-2 infection did not significant alter TJ mRNA expression (data not shown).

SARS-CoV-2 productively infects the bronchial epithelial cell line, Calu-3, and pNECs from healthy controls

We further investigated the impact of FP on SARS-CoV-2 infection. Therefore, infection efficiency of SARS-CoV-2 was first determined on ALI cultures of both Calu-3 cells and pNECs. Apical washes at one- and three-days post infection were collected and subjected to RNA extraction and RT-qPCR analysis of viral nucleocapsid (N) copies. Virus yield analysis showed that ALI cultures of Calu-3 cells were successfully infected with SARS-CoV-2 (Figure 2A), as evidenced by the high viral RNA copy numbers in the apical washes at 72 hours post infection that exceeded the amount of virus input at time of infection. Microscopic images were taken at subsequent days post infection to verify that there was indeed a successful infection of the ALI Calu-3 cell cultures

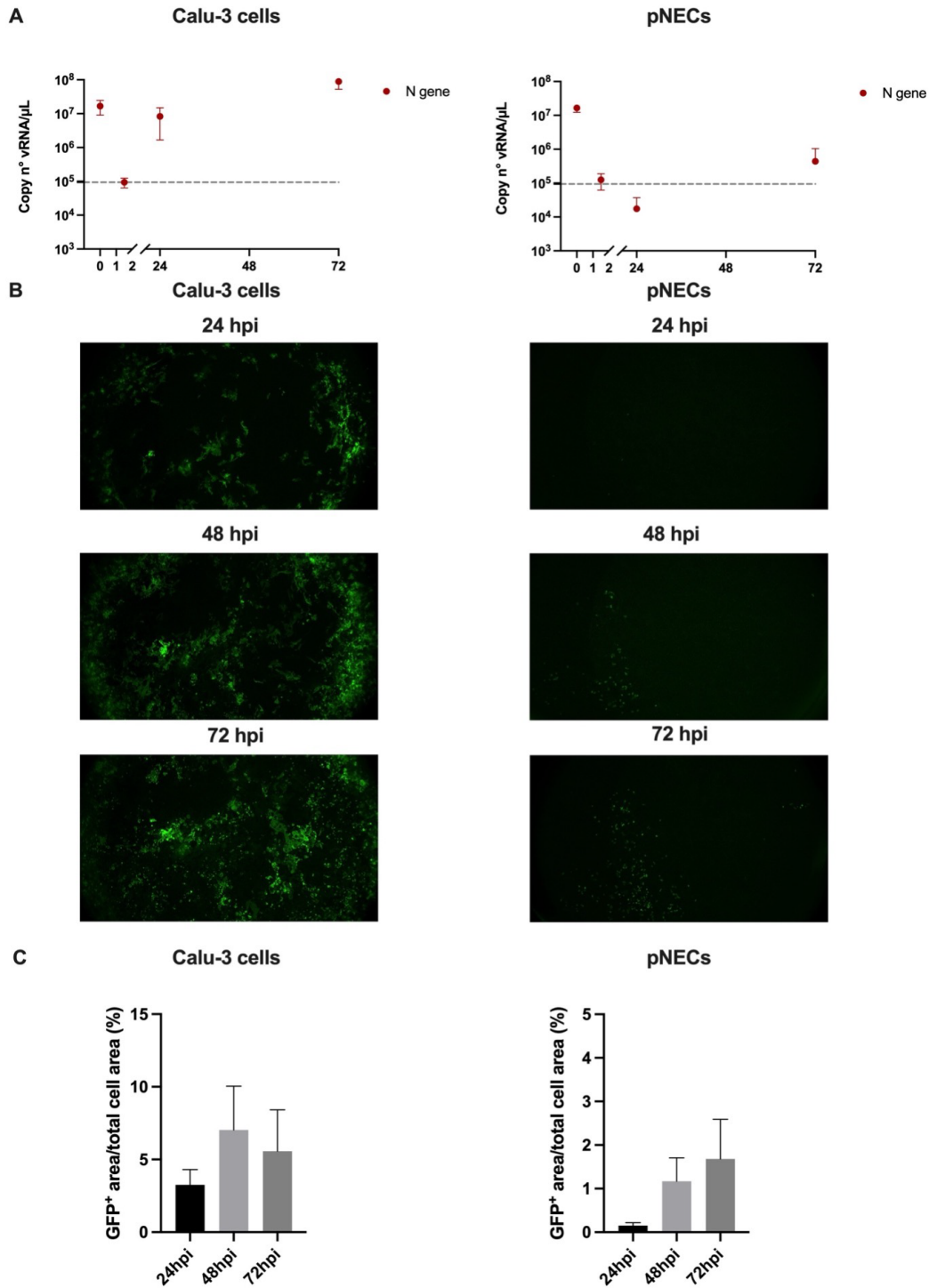


Figure 2. SARS-CoV-2 successfully infects Calu-3, and pNECs from healthy controls. A: Apical viral release over time of Calu-3 cells (left) and pNECs (right). B: Representative fluorescent microscopy images (4X objective) of viral infection in Calu-3 cells (left) and pNECs (right) at 24, 48 and 72 hours post infection with a GFP-expressing SARS-CoV-2 variant. C: Quantification of viral infection in Calu-3 cells (left) and pNECs (right) showing the percentage of the GFP⁺ area to the total cell area over time. Data are mean \pm SD from four independent experiments. Images are representative of four independent experiments.

with a GFP-expressing SARS-CoV-2 variant (Figure 2B). As the GFP gene is introduced in the viral genome of the recombinant SARS-CoV-2, only infected cells that replicate virus do express

GFP. In Calu-3 cells, a profound infection with SARS-CoV-2 was obtained within 24 hours, and levels of GFP further increased over time (Figure 2C), confirming a productive viral replication

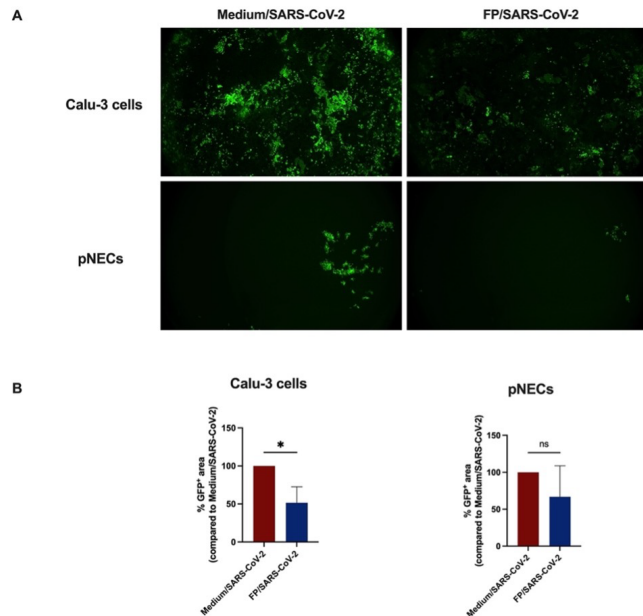


Figure 3. FP shows anti-viral effect against SARS-CoV-2 infection in vitro. Cells were basolaterally pretreated with FP (0,1 μ M) for 48 hours and subsequently apically exposed to a GFP-expressing SARS-CoV-2 variant for 2 hours. A.: Representative fluorescent microscopic images (4X objective) of ALI cultures of Calu-3 cells (upper panels) and pNECs (lower panels) from healthy controls at three days post infection (n=4). ALI cultures were either non-treated (medium/SARS-CoV-2; left panels) or pre-treated with FP for 48 hours (FP/SARS-CoV-2; right panels). As the GFP gene is introduced in the viral genome of the recombinant SARS-CoV-2, only infected cells that replicate virus do express GFP. pNECs = primary nasal epithelial cells; FP = fluticasone propionate. B: Quantification of non-treated (Medium/SARS-CoV-2) or pre-treated (FP/SARS-CoV-2) conditions, showing the percentage of the GFP+ area compared to non-treated infected control condition. Data are mean \pm SD (n = 4). Statistical analysis was performed using paired t test; * P < 0.05, ns = not significant.

in the Calu-3 cells. SARS-CoV-2 infection of pNECs was less efficient, though, active viral replication could be observed at 72 hours post infection, as evidenced by progressively increasing levels of GFP expression (Figure 2C) and by detectable viral RNA copies in the apical washes (Figure 2A, right panel). In parallel, virus release in the basolateral medium was analyzed, and confirmed that the differentiated Calu-3 cells were more prone to SARS-CoV-2 infection than the pNECs (Figure E1).

Fluticasone propionate shows anti-viral effects against SARS-CoV-2 infection of ALI cultures

We then tested the preventive effect of FP on SARS-CoV-2 infection in our ALI cultures. Cells were pre-treated with FP for 48 hours before exposure to SARS-CoV-2. Pre-treatment of ALI cultures with FP resulted in a modest but meaningful (a

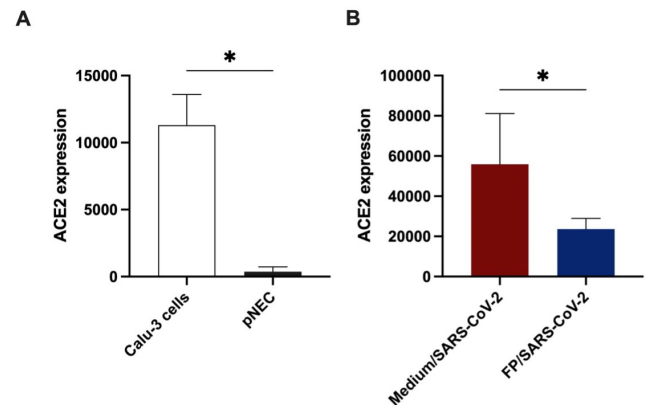


Figure 4. FP suppresses ACE2 expression in SARS-CoV-2 infected Calu-3 cells. A: mRNA expression of ACE2 in ALI-cultures of Calu-3 cells (n=4) and pNECs (n=4). Relative mRNA expression versus the housekeeping genes encoding hRACK1 and hPPIA are shown. B: mRNA expression of ACE2 in ALI cultures of Calu-3 cells (n=4) after pre-treatment with FP (for 48 hours) and infection with SARS-CoV-2. Samples were collected at 72 hours post infection. Data are shown as mean \pm SD. Significance was calculated using one-way ANOVA. *P<0.05. pNECs = primary nasal epithelial cells; FP = fluticasone propionate. hpi = hours post infection.

difference of 0.51 log₁₀ viral RNA copy numbers/ μ L, P < 0.02) decrease of virus release in the apical washes of Calu-3 cells at 24 hours post infection (data not shown). At this early time point post infection, no productive virus release was obtained in the basolateral medium. Also, at three days post infection (endpoint measurement of experiment), decreased levels of GFP expression was observed in FP-treated SARS-CoV-2 infected Calu-3 cells, not only microscopically (Figure 3A), but also the GFP quantification revealed a significant reduced GFP expression of 48.32% (P < 0.05) in the FP-treated samples compared to the non-treated control infected condition (Figure 3B). Of note, pre-treatment with FP did not alter the apical nor basolateral release of SARS-CoV-2 viral particles produced by pNECs (data not shown). Although, FP clearly reduced the rather weak GFP expression in pNECs at three days post infection (Figure 3A, B), it did not reach significance (P > 0.05).

Fluticasone propionate suppresses ACE2 expression in SARS-CoV-2 infected Calu-3 cells

The respiratory tract is continuously exposed to various environmental substances, making it a primary target for SARS-CoV-2 to enter and infect the human body. Indeed, SARS-CoV-2 relies heavily on ACE2 and TMPRSS2 expressed on nasal epithelial cells for cell entry⁽¹¹⁾. Therefore, we next compared the basal expression of ACE2 between ALI-cultures of Calu-3 cells and pNECs (Figure 4A). Interestingly, we measured a significant higher expression of ACE2 in Calu-3 cells compared to pNECs (Figure 4A), which might explain that, in our experimental setting, Calu-

3 cells can be more easily infected with SARS-CoV-2 compared to pNECs (Figure 2B). Next, we investigated the effect of FP pretreatment on ACE2 expression in SARS-CoV-2 infected Calu-3 cells. FP treatment of infected Calu-3 cells significantly reduced the expression of ACE2 (Figure 4B).

Discussion

The ongoing COVID-19 pandemic has stimulated to quickly increase our scientific knowledge about the pathophysiology and potential means of prevention and treatment. Research has shown that the human respiratory epithelium is the primary target of SARS-CoV-2⁽⁶⁾. Moreover, the direct and indirect effects of SARS-CoV-2 on the respiratory epithelium, and the severity of such process can lead to detrimental anatomical and structural damages, respiratory distress syndrome and even death⁽²⁴⁾. As such, understanding the regulation of SARS-CoV-2 cell entry is important, as it can directly lead to the study and development of preventive and therapeutic strategies against COVID-19⁽²⁾. Initial focus has been mainly on the lower airways, rather than on the upper airways⁽²⁵⁻²⁾. However, since the sinonasal cavity is an interface between the environment and the respiratory tract, and high SARS-CoV-2 viral loads can be detected in nasal swabs from infected patients, we focused in our current study on the effect of SARS-CoV-2 infection (Wuhan strain) on the upper respiratory tract⁽²⁸⁾. Here, we show that SARS-CoV-2 can successfully infect pNECs from healthy controls as well as Calu-3 cells. This successful infection is potentially due to ACE2 expression on various cell types present in both the upper and lower airways⁽²⁹⁾. Indeed, our data showed expression of ACE2 on Calu-3 cells as well as on pNECs. However, the expression of ACE2 in pNECs from healthy controls was rather low compared to Calu-3 cells, which can explain the lower SARS-CoV-2 infection efficiency in pNECs. The later might also explain why FP did not alter the apical nor basolateral release of SARS-CoV-2 viral particles produced by pNECs. The lower SARS-CoV-2 infection efficiency in pNECs is as such a limitation of this study. Additionally, in the study of Bezara et al., the authors demonstrated that the expression of ACE2 in the upper respiratory tract can vary regionally, based on the characteristics of the epithelium. More specifically, they showed ACE2 mRNA transcripts in 2-6% of epithelial cells, by means of scRNA-sequencing, with rare detection in thicker ciliated pseudostratified epithelium, and more abundant ACE2 proteins in thinner epithelium⁽²⁹⁾. These findings might also explain the lower expression of ACE2 in our pNECs.

Another highlight of this study was the suppressive effect of FP on SARS-CoV-2 infection in ALI cultures of Calu-3 cells and pNECs. Moreover, FP pretreatment was able to suppress SARS-CoV-2 induced increase in epithelial permeability in Calu-3 cells. From a clinical point of view, controversy remains for the use of corticosteroids for COVID-19^(30,31). Although clinical evidence

does not support systemic corticosteroid treatment for COVID-19⁽³⁰⁾, ciclesonide and mometasone, two widely used ICS, showed beneficial effects against SARS-CoV-2 replication in vitro⁽³²⁾. As for intra-nasal corticosteroids, Strauss and colleagues demonstrated that usage of intra-nasal corticosteroids was associated with a lower risk for COVID-19-related hospitalization, ICU admission and hospital mortality⁽¹⁶⁾. However, these corticosteroids might impair anti-viral immune responses and increase viral titers, as has been reported for rhinovirus infection⁽³³⁾. Nevertheless, clinical studies are warranted to confirm the clinical efficacy of FP, and of corticosteroids in general, in preventing SARS-CoV-2 infection in vivo. Interestingly, we also demonstrated that FP down-modulates ACE2 expression, which in turn can be related to reduced viral entry and the observed antiviral effect of FP. These results are in line with previous data⁽²⁰⁾ on inhaled corticosteroids reducing the expression of ACE2 in epithelial cells through the suppression of Type-I interferon response, hence contributing to altered susceptibility to SARS-CoV-2 infection. However, it remains unknown whether the partial suppression of ACE2 expression by FP can indeed fully prevent SARS-CoV-2 spreading. In addition, another limitation of our study is the administration route of FP. Because of a methodological necessity, FP was not applied apically but basolaterally, thus, in a non-physiological manner.

Lastly, we investigated the effect of SARS-CoV-2 infection on TJ expression (i.e., occludin, zonula occludens-1, claudin-1, -3 and -4) in Calu-3 cells 72 hours post infection. We found that SARS-CoV-2 infection did not alter TJ mRNA expression. This was somewhat surprising as previous studies reported an effect of SARS-CoV-2 infection on TJ expression^(8,34). Yet, it could be that the organization of the TJs is compromised, which cannot be seen on mRNA level. In addition, differences in cell type and SARS-CoV-2 infection time and concentration, might also explain these discrepancies. Nevertheless, the importance of the nasal epithelial barrier in SARS-CoV-2 infection may not be underestimated and should be of greater focus in the COVID-19 research.

Conclusions

Taken together, we could demonstrate that pretreatment with FP can prevent SARS-CoV-2 viral replication and suppress epithelial barrier dysfunction, together with the reduced expression of ACE2. The ability of intranasal corticosteroids to protect the epithelial barrier against harmful substances has already been demonstrated in several in vitro and in vivo models^(18,19). Therefore, we believe that our in vitro data will contribute to the start up of additional clinical studies to demonstrate the potential of intranasal corticosteroids as a novel SARS-CoV-2 antiviral treatment.

Acknowledgements

Katleen Martens is supported by a Postdoctoral Fellowship of the Fund of Scientific Research (FWO, 12Z0622N), Flanders, Belgium. Brecht Steelant is supported by a Postdoctoral Fellowship of the Fund of Scientific Research (FWO, 12U6721N), Flanders, Belgium. Peter Hellings received a senior researcher fellowship from the Fund of Scientific Research (FWO), Flanders, Belgium. The authors would like to thank Ellen Dilissen, Becky Provinciael, Anita Camps and Joren Stroobants for their insightful comments and technical advice, Prof. Dr. Mark Jorissen and Prof. Dr. Laura Van Gerven (UZ Leuven) for collecting nasal tissue.

Authorship contribution

KM, EV, and AV performed experiments, acquired data, analy-

zed data and wrote the manuscript. BS, PWH and KV discussed and interpreted findings, and critically revised the manuscript. PWH and KV designed research study and critically revised the manuscript.

Conflicts of interest

The authors declare no competing interest related to this work.

Funding

KM and BS are currently Postdoctoral Fellows of the Fund for Scientific Research Flanders (FWO), Flanders, Belgium. PWH is a recipient of a senior researcher fellowship from the FWO. This work was supported by an unrestricted grant of GSK.

References

- Chan JF, Yuan S, Kok KH, et al. A familial cluster of pneumonia associated with the 2019 novel coronavirus indicating person-to-person transmission: a study of a family cluster. *Lancet*. 2020 Feb 15;395(10223):514-523.
- Wu F, Zhao S, Yu B, et al. A new coronavirus associated with human respiratory disease in China. *Nature*. 2020 Mar;579(7798):265-269. Erratum in: *Nature*. 2020 Apr;580(7803):E7.
- Planas D, Saunders N, Maes P, et al. Considerable escape of SARS-CoV-2 Omicron to antibody neutralization. *Nature* 602, 671–675 (2022).
- Jean SS, Lee PI, Hsueh PR. Treatment options for COVID-19: The reality and challenges. *J Microbiol Immunol Infect*. 2020 Jun;53(3):436-443.
- Sanders JM, Monogue ML, Jodlowski TZ, Cutrell JB. Pharmacologic Treatments for Coronavirus Disease 2019 (COVID-19): A Review. *JAMA*. 2020 May 12;323(18):1824-1836.
- Hanchard J, Capó-Vélez CM, Deusch K, Lidington D, Bolz SS. Stabilizing Cellular Barriers: Raising the Shields Against COVID-19. *Front Endocrinol (Lausanne)*. 2020 Sep 30;11:583006.
- Hellings PW, Steelant B. Epithelial barriers in allergy and asthma. *J Allergy Clin Immunol*. 2020 Jun;145(6):1499-1509.
- Hao S, Ning K, Kuz CA, Vorhies K, Yan Z, Qiu J. Long-Term Modeling of SARS-CoV-2 Infection of In Vitro Cultured Polarized Human Airway Epithelium. *mBio*. 2020 Nov 6;11(6):e02852-20.
- Smallcombe CC, Linfield DT, Harford TJ, et al. Disruption of the airway epithelial barrier in a murine model of respiratory syncytial virus infection. *Am J Physiol Lung Cell Mol Physiol*. 2019 Feb 1;316(2):L358-L368.
- Rezaee F, DeSando SA, Ivanov AI, Chapman TJ, Knowlton SA, Beck LA, Georas SN. Sustained protein kinase D activation mediates respiratory syncytial virus-induced airway barrier disruption. *J Virol*. 2013 Oct;87(20):11088-95.
- Rezaee F, Georas SN. Breaking barriers. New insights into airway epithelial barrier function in health and disease. *Am J Respir Cell Mol Biol*. 2014 May;50(5):857-69.
- Sungnak W, Huang N, Bécavin C, et al. SARS-CoV-2 entry factors are highly expressed in nasal epithelial cells together with innate immune genes. *Nat Med*. 2020 May;26(5):681-687.
- Ziegler CGK, Allon SJ, Nyquist SK, et al. SARS-CoV-2 Receptor ACE2 Is an Interferon-Stimulated Gene in Human Airway Epithelial Cells and Is Detected in Specific Cell Subsets across Tissues. *Cell*. 2020 May 28;181(5):1016-1035.e19.
- Hoffmann M, Kleine-Weber H, Schroeder S, et al. SARS-CoV-2 cell entry depends on ACE2 and TMPRSS2 and is blocked by a clinically proven protease inhibitor. *Cell*. 2020 Apr 16;181(2):271-280.e8.
- Radzikowska U, Ding M, Tan G, et al. Distribution of ACE2, CD147, CD26, and other SARS-CoV-2 associated molecules in tissues and immune cells in health and in asthma, COPD, obesity, hypertension, and COVID-19 risk factors. *Allergy*. 2020 Nov;75(11):2829-2845.
- Strauss R, Jawhari N, Attaway AH, et al. Intranasal Corticosteroids Are Associated with Better Outcomes in Coronavirus Disease 2019. *J Allergy Clin Immunol Pract*. 2021 Nov;9(11):3934-3940.e9.
- Calverley PM, Page C, Dal Negro RW, et al. Effect of Erdosteine on COPD Exacerbations in COPD Patients with Moderate Airflow Limitation. *Int J Chron Obstruct Pulmon Dis*. 2019 Dec 2;14:2733-2744.
- Steelant B, Farré R, Wawrzyniak P, et al. Impaired barrier function in patients with house dust mite-induced allergic rhinitis is accompanied by decreased occludin and zonula occludens-1 expression. *J Allergy Clin Immunol*. 2016 Apr;137(4):1043-1053.e5.
- Doulaptsi M, Wils T, Hellings PW, et al. Mometasone furoate and fluticasone furoate are equally effective in restoring nasal epithelial barrier dysfunction in allergic rhinitis. *World Allergy Organ J*. 2021 Sep 11;14(9):100585.
- Finney LJ, Glanville N, Farne H, et al. Inhaled corticosteroids downregulate the SARS-CoV-2 receptor ACE2 in COPD through suppression of type I interferon. *J Allergy Clin Immunol*. 2021 Feb;147(2):510-519.e5.
- Vanhulle E, Provinciael B, Stroobants J, Camps A, Maes P, Vermeire K. Intracellular flow cytometry complements RT-qPCR detection of circulating SARS-CoV-2 variants of concern. *BioRxiv*. 2022.
- Thi Nhu Thao T, Labrousseau F, Ebert N, et al. Rapid reconstruction of SARS-CoV-2 using a synthetic genomics platform. *Nature*. 2020 Jun;582(7813):561-565.
- Schindelin J, Arganda-Carreras I, Frise E, et al. Fiji: an open-source platform for biological-image analysis. *Nat Methods*. 2012 Jun 28;9(7):676-82.
- Mohanty SK, Satapathy A, Naidu MM, et al. Severe acute respiratory syndrome coronavirus-2 (SARS-CoV-2) and coronavirus disease 19 (COVID-19) - anatomic pathology perspective on current knowledge. *Diagn Pathol*. 2020 Aug 14;15(1):103.
- Li G, He X, Zhang L, et al. Assessing ACE2 expression patterns in lung tissues in the pathogenesis of COVID-19. *J Autoimmun*. 2020 Aug;112:102463.
- Lukassen S, Chua RL, Trefzer T, et al. SARS-CoV-2 receptor ACE2 and TMPRSS2 are primarily expressed in bronchial transient secretory cells. *EMBO J*. 2020 May 18;39(10):e105114.
- Pinto BGG, Oliveira AER, Singh Y, et al. ACE2 Expression Is Increased in the Lungs of Patients With Comorbidities Associated With Severe COVID-19. *J Infect Dis*. 2020 Jul 23;222(4):556-563.
- Wang W, Xu Y, Gao R, et al. Detection of SARS-CoV-2 in Different Types of Clinical Specimens. *JAMA*. 2020 May 12;323(18):1843-1844.
- Ortiz Bezara ME, Thurman A, Pezzulo AA, et

- al. Heterogeneous expression of the SARS-Coronavirus-2 receptor ACE2 in the human respiratory tract. *bioRxiv* [Preprint]. 2020 Aug 13:2020.04.22.056127.
30. Russell, B., Moss, C., Rigg, A., & Van Hemelrijck, M. (2020). COVID-19 and treatment with NSAIDs and corticosteroids: should we be limiting their use in the clinical setting?. *Ecancermedalscience*, 14, 1023.
31. Shang L, Zhao J, Hu Y, Du R, Cao B. On the use of corticosteroids for 2019-nCoV pneumonia. *Lancet*. 2020 Feb 29;395(10225):683-684.
32. Matsuyama S, Kawase M, Nao N, et al. The Inhaled Steroid Ciclesonide Blocks SARS-CoV-2 RNA Replication by Targeting the Viral Replication-Transcription Complex in Cultured Cells. *J Virol*. 2020 Dec 9;95(1):e01648-20.
33. Singanayagam A, Glanville N, Bartlett N, Johnston S. Effect of fluticasone propionate on virus-induced airways inflammation and anti-viral immune responses in mice. *Lancet*. 2015 Feb 26;385 Suppl 1:S88.
34. Zhu N, Wang W, Liu Z, et al. Morphogenesis and cytopathic effect of SARS-CoV-2 infection in human airway epithelial cells. *Nat Commun*. 2020 Aug 6;11(1):3910.

Prof. Dr. Peter Hellings
Research group Allergy and Clinical Immunology
Department of Microbiology Immunology and Transplantation
KU Leuven
Herestraat 49 – box 811
3000 Leuven
Belgium

Tel.: +32 16 33 23 38
E-mail: peter.hellings@kuleuven.be

SUPPLEMENTARY MATERIAL

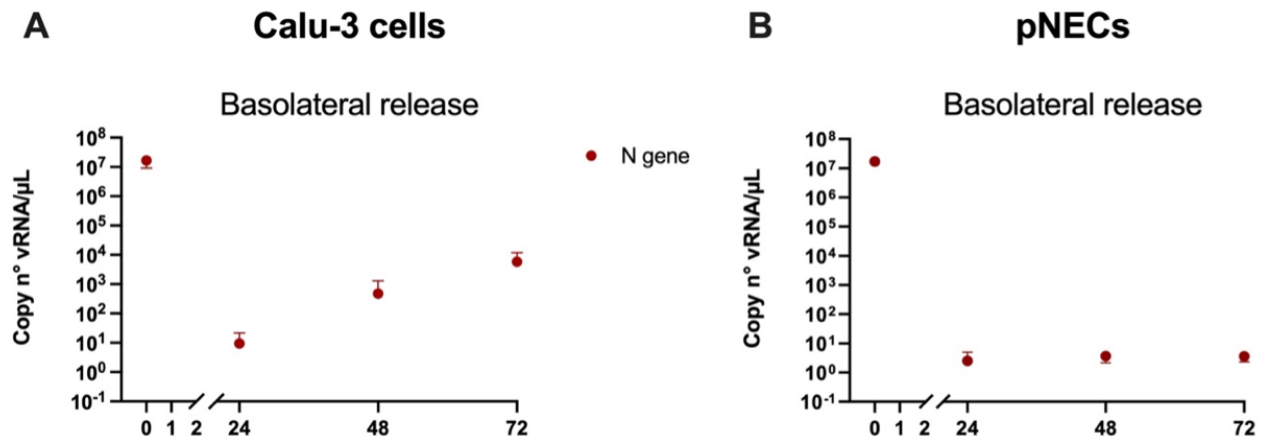


Figure S1. Basolateral viral release over time of Calu-3 cells (A) and pNECs (B).

Table S1. Patient's demographics.

N	Controls
	4
Age (mean ± SD)	29,2 ± 17,95
Gender (male/female)	3/2
Allergy (%)	0%
Intranasal steroids (%)	0%
Smoking (%)	0%

Table S2. Primer and probe sequences used in RT-qPCR.

Primer/Probe	Sequence	Reference
SC2*N-fw	ttacaacattggccgcaaa	US CDC
SC2N-rv	gcgcgacattccgaagaa	US CDC
SC2N Probe	Fam-acaattgccccagcgcttcag(bhq1)	US CDC
SC2E-fw	acaggtacgtaaatagtaaatagcgt	DE Charité
SC2E-rev	atattgcagcagtagcacaca	DE Charité
SC2 E Probe	Hex-acactagcc(zen)atccttactgcgcttcg(31abkfq)	DE Charité
PPIA-fw	cgc gtc tcc ttt gag ctg tt	
PPIA-rv	ctg aca cat aaa ccc tgg aat aat tc	
PPIA-tp	cag aca agg tcc caa aga cag cag aaa att t	5'Fam3'Tamra
RACK1-fw	cac tgt cca gga tga gag cca	
RACK1-rv	cat acc ttg acc agc ttg tcc c	
RACK1-tp	tcc gct tct cg cca aca gca g	5'Fam3'Tamra
ACE2-fw	gga gat gaa gcg aga gat agt tgg	
ACE2-rv	att aga aac atg gaa cag aga tgc g	
ACE2-tp	tgg tgg aac ctg tgc ccc atg at	5'Fam3'Tamra